UC Davis
UC Davis Previously Published Works

Title

Inducible CRISPR-targeted knockdown of human gut Bacteroides in gnotobiotic mice discloses glycan utilization strategies.

Permalink

Journal

Authors

Beller, Zachary
Wesener, Darryl
Seebeck, Timothy
et al.

Publication Date

DOI

Peer reviewed

Inducible CRISPR-targeted "knockdown" of human gut *Bacteroides* in gnotobiotic mice discloses glycan utilization strategies

Zachary W. Beller[a,b] ID, Darryl A. Wesener[a,b], Timothy R. Seebeck[a,b,c], Janaki L. Guruge[a,b], Alexandra E. Byrne[a,b], Suzanne Henrissat[a,b,d], Nicolas Terrapon[d], Bernard Henrissat[e,f], Dmitry A. Rodionov[g], Andrei L. Osterman[g], Chris Suarez[h], Nikita P. Bacalzo Jr.[h], Ye Chen[h], Garret Couture[h], Carlito B. Lebrilla[h] ID, Zhigang Zhang[c], Erik R. Eastlund[c], Caitlin H. McCann[c], Gregory D. Davis[c], and Jeffrey I. Gordon[a,b,1]

Understanding how members of the human gut microbiota prioritize nutrient resources is one component of a larger effort to decipher the mechanisms defining microbial community robustness and resiliency in health and disease. This knowledge is foundational for development of microbiota-directed therapeutics. To model how bacteria prioritize glycans in the gut, germfree mice were colonized with 13 human gut bacterial strains, including seven saccharolytic *Bacteroidaceae* species. Animals were fed a Western diet supplemented with pea fiber. After community assembly, an inducible CRISPR-based system was used to selectively and temporarily reduce the absolute abundance of *Bacteroides thetaiotaomicron* or *B. cellulosilyticus* by 10- to 60-fold. Each knockdown resulted in specific, reproducible increases in the abundances of other *Bacteroidaceae* and dynamic alterations in their expression of genes involved in glycan utilization. Emergence of these "alternate consumers" was associated with preservation of community saccharolytic activity. Using an inducible system for CRISPR base editing in vitro, we disrupted translation of transporters critical for utilizing dietary polysaccharides in *Phocaeicola vulgatus*, a *B. cellulosilyticus* knockdown-responsive taxon. In vitro and in vivo tests of the resulting *P. vulgatus* mutants allowed us to further characterize mechanisms associated with its increased fitness after knockdown. In principle, the approach described can be applied to study utilization of a range of nutrients and to preclinical efforts designed to develop therapeutic strategies for precision manipulation of microbial communities.

human gut microbiome | polysaccharide utilization | community ecology/interbacterial interactions | CRISPR mutagenesis | gnotobiotic mice

Processing of dietary polysaccharides is a task that is "outsourced" to our gut microbiomes. Our human genome encodes 97 glycoside hydrolases and no polysaccharide lyases, with fewer than 20% targeting structures from dietary glycans (1). In contrast, our microbiomes contain tens of thousands of these genes, and a single gut bacterial strain can have dozens of different families of glycoside hydrolases (GH) and polysaccharide lyases (PL) (1, 2). This arsenal of microbial carbohydrate active enzymes (CAZymes) is responsible for degrading dietary glycan structures, which represent a large combinatorial space of monosaccharides, glycosidic linkages, branching patterns, and modifications.

Human gut *Bacteroidaceae* are prevalent primary consumers of fiber glycans; as such, they provide an attractive model to address mechanistic questions about nutrient resource allocation in the gut microbiota. *Bacteroidaceae* genomes are replete with CAZymes, the majority of which are organized into supraoperonic gene clusters called polysaccharide utilization loci (PULs). PULs represent functional units responsible for utilizing different types of glycan structures; they encode extracellular and intracellular CAZymes that degrade larger glycans, SusC- and SusD-like proteins that bind and import glycan fragments generated by pericellular degradation, and transcription factors that sense a carbohydrate-derived epitope and regulate the locus (3). In principle, the CAZymes encoded within a bacterial genome and their expression levels can be used to infer the glycans utilized by that organism. However, comparative genomic analyses and in vitro growth assays have emphasized that different *Bacteroidaceae* often possess overlapping abilities to utilize polysaccharides, complicating the prediction of glycan allocation in a microbial community context (4, 5).

In the simplest case when a single nutrient resource is available, one might predict that the organism with a fitness advantage in that nutrient context wins out (6). However, it is less obvious what will occur in a gut ecosystem rich in alternative nutrient resources and populated by diverse, potentially highly competitive microbes. Many bacteria employ "diauxie"; i.e., they maximize their growth via sequential utilization of available nutrient

Significance

Learning how human gut bacteria compete and cooperate to metabolize nutrients is an important step toward developing more nutritious foods and promoting healthier gut microbial communities. Human gut *Bacteroidaceae* are primary consumers of complex dietary polysaccharides. Here, we describe a genetic system for deliberately inducing a decrease in the abundance of a target organism in a gut community. Gnotobiotic mice were fed a human diet and colonized with a defined community of cultured, genome-sequenced, human gut bacteria, including multiple *Bacteroidaceae* species. "Knockdowns" of different *Bacteroides* within the established community resulted in specific increases in the abundances of other organisms and revealed how they dynamically changed their priorities for utilizing available polysaccharides while preserving the community's overall capacity to metabolize carbohydrates.

resources (7). Diauxie was classically demonstrated for monosaccharides, and recently for *Bacteroidaceae* in the context of polysaccharide mixtures (8, 9). When these sequential patterns of resource utilization differ between species, or if organisms have distinct dynamic patterns of utilization (e.g., fast resource switching), multiple species can thrive together even when one organism might be dominant in the context of each single nutrient resource (9, 10). In addition, during in vivo growth or in vitro growth in mixed cultures, bacteria may profit from "public goods" that are provided by their neighbors' catabolism of otherwise inaccessible nutrient sources (11, 12). These considerations illustrate the complexity faced when trying to define the mechanisms that underlie nutrient utilization by human gut microbial communities and the factors that contribute to inter- and intrapersonal variations observed in microbiota (and host) responses in clinical studies that involve fiber-supplemented diets (e.g., refs. 13 and 14).

We have previously modeled glycan utilization by introducing defined consortia of cultured human gut bacteria into germfree mice. Mice were fed a diet representing the upper tertile of saturated fat consumption and the lower tertile of fruit and vegetable consumption in the NHANES database of dietary practices in the United States (15), with or without supplementation with different plant fiber preparations. By documenting the effects of the fibers on the fitness (abundances) of consortium members and their patterns of gene expression, we could infer their glycan utilization patterns. Whole genome transposon mutagenesis disclosed specific loci, notably components of PULs, that were key determinants of the fitness of fiber responsive *Bacteroidaceae* (16, 17). Additionally, glycan utilization was directly audited by oral gavage of paramagnetic microscopic glass beads composed of glycans covalently linked to the particle surface (17–19). Different types of these "artificial food particles" (or microbiota functional activity biosensors; MFABs), each containing a given glycan preparation and a unique fluorophore "barcode," were administered simultaneously: Beads were then retrieved from feces or different regions of the intestine (by magnetism), purified (by FACS), and finally community saccharolytic activity was quantified by mass spectrometry of their glycan content (17–19).

We have applied this approach to study a pea fiber preparation that was later incorporated into the human snack food prototypes (13). A principal bioactive component of this fiber preparation was isolated: It consists predominantly of a 2-*O*-branched arabinan attached to small rhamnogalacturonan-I pectic fragments (2-substituted and 2,4-substituted rhamnose) and small galactan oligomers (4-substituted galactose), plus linear xylan (4-substituted xylose) and glucose (in the form of residual starch) (19). Studies in gnotobiotic mice colonized with a defined consortium of cultured, genome-sequenced human gut bacteria showed that adding either unfractionated pea fiber or this purified pea fiber arabinan fraction to the high saturated fat, low fruit and vegetable (HiSF-LoFV) diet selectively increased the abundances of a subset of *Bacteroidaceae* present in the community. Omitting *B. cellulosilyticus*, an organism with arabinoxylan-processing PULs, from the consortium prior to colonization revealed one way that *B. ovatus* avoids competition between itself and *B. cellulosilyticus*; namely, that *B. ovatus* expresses its arabinoxylan processing PULs at lower levels when *B. cellulosilyticus* is present and at significantly higher levels when *B. cellulosilyticus* is absent (17).

While these types of "leave one or more organisms out" experiments represent a way for modeling nutrient prioritization/utilization by members of the human gut microbiota, they fail to capture the dynamic behavior of a previously established community as it responds to perturbation. In contrast, deliberately inducing a decrease in the abundance ("knockdown") of a target

organism in an established defined community offers an opportunity to characterize mechanisms underlying community adaptations in the context of a given diet and the timescales over which these adaptations operate. One approach for achieving this type of perturbation has been to use phage to attack human gut bacteria represented in a defined community established in gnotobiotic mice (e.g., refs. 20 and 21). In the current study, we use another approach that targeted either *B. thetaiotaomicron* or *B. cellulosilyticus* in an established 13-member model human gut microbiota containing a total of seven species of *Bacteroidaceae*. *B. thetaiotaomicron* or *B. cellulosilyticus* strains were engineered to contain a genetically integrated "kill-switch" composed of an inducible, self-targeting SpCas9 that functions by creating deleterious double-stranded breaks in the bacterial chromosome (22). The effects of inducing a knockdown of the targeted *Bacteroides* strain on the absolute abundances of other consortium members were defined in mice consuming the HiSF-LoFV diet supplemented with pea fiber. Changes in gene expression within community members were delineated using microbial RNA-Seq. Community saccharolytic activity was measured by mass spectrometry of retrieved MFABs as well as residual glycans present in cecal contents. Additionally, our genetic system was adapted for Cas9-cytidine deaminase mutagenesis (23, 24) and used to disrupt the translation of genes associated with the response of *Phocaeicola vulgatus* (previously known as *Bacteroides vulgatus*) to *B. cellulosilyticus* knockdown. The effects of *B. cellulosilyticus* knockdown on the fitness and patterns of gene expression of these *P. vulgatus* mutants were examined over time to further define the mechanisms by which these two taxa and other members of the community interact and compete for glycans.

Results

Knockdown Strains. Work in multiple bacterial species has demonstrated that expressing Cas9 nuclease along with a guide RNA (gRNA) targeting the bacterial chromosome is lethal, likely due to irreparable genomic lesions (25, 26). While attempts have been made to leverage this bactericidal activity to eliminate pathogenic and antibiotic-resistant bacteria (26–28), we reasoned that this tool could be adapted for depleting the absolute abundances of targeted *Bacteroides* in gnotobiotic mice colonized with a defined consortium of human gut bacteria. Given our previous studies described in the *Introduction* section, we targeted *B. cellulosilyticus* WH2 and *B. thetaiotaomicron* VPI-5482 for these knockdown experiments.

To construct strains of these two organisms for inducible expression of Cas9, we employed a pNBU2 integration plasmid (29) containing i) a *SpCas9* gene driven by a tetracycline-inducible promoter (30), ii) a constitutively expressed, self-targeting gRNA or a control scrambled gRNA, and iii) an antibiotic selection marker (erythromycin [*ermG* in the case of *B. thetaiotaomicron* or cefoxitin [*cfxA*] in the case of *B. cellulosilyticus* WH2) (Fig. 1*A*, *SI Appendix*, Fig. S1 *A* and *B*, and Dataset S1A). Engineered strains possessed a scrambled gRNA (denoted as BT-M1 or BC-M1), a gRNA targeting a *susC*-like gene (BT-S# or BC-S#), or a *tdk*-targeted gRNA (BT-T# or BC-T#). When plated on Brain Heart Infusion (BHI) medium containing anhydrotetracycline (aTc), a tetracycline derivative without antibiotic activity, the viability of strains with the self-targeting gRNA decreased by 10^3 to 10^5-fold compared to cells plated on medium lacking aTc (triplicate cultures/strain; $P < 0.05$; two-way ANOVA, Tukey's HSD; *SI Appendix*, Fig. S1*C*). In contrast, aTc produced no statistically significant reduction in the number of colony-forming units (cfu) of strains containing the scrambled gRNA. Tests of two strains containing two distinct self-targeting
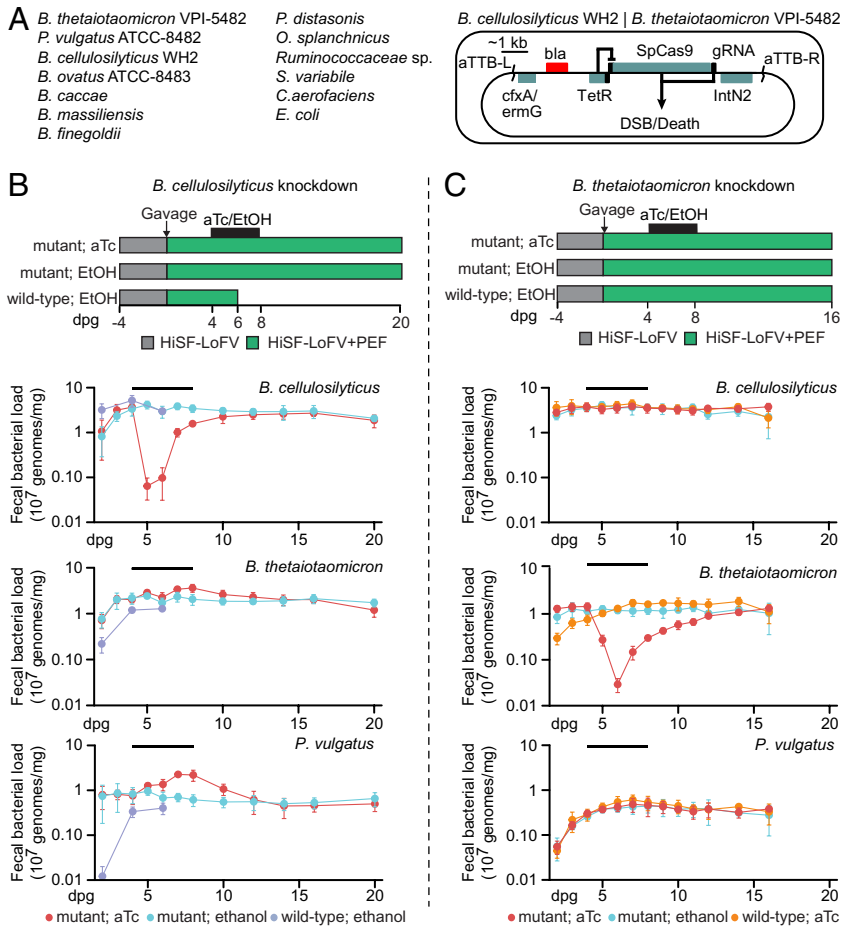
Fig. 1. Knockdown of *B. cellulosilyticus* and *B. thetaiotaomicron* from a defined community. (*A*) Human gut bacterial consortium and diagram of CRISPR knockdown cassette. Knockdown strains were constructed by integration of a pNBU2-based vector containing an aTc-inducible SpCas9 gene and constitutively expressed gRNA, which complex to create genomic double-stranded breaks (DSB). (*B*) Experimental design of *B. cellulosilyticus* knockdown. Germfree mice were fed the HiSF-LoFV diet for 4 d and then colonized with a 13-member consortium containing the *B. cellulosilyticus* wild-type (WT) or knockdown mutant strain (BC-S19). After gavage, mice were monotonously fed a HiSF-LoFV diet supplemented with 10% (w/w) pea fiber (PEF) ad libitum and treated with aTc or ethanol in their drinking water from dpg 4 to 8. Absolute abundances of the indicated community members were defined in serially collected fecal samples. Mean values ± SD are shown (n = 5 to 10 mice/treatment group). (*C*) Experimental design of *B. thetaiotaomicron* knockdown. Mice were colonized with a 13-member bacterial consortium containing the wild-type (WT) or a knockdown mutant strain (BT-T1). Absolute abundances of the indicated community members are shown (mean ± SD; n = 5 to 10/treatment group).

gRNA sequences for each organism revealed only modest effects of the different gRNAs on the magnitude of reduction in cfu for each *Bacteroides* species (mean marginal difference = threefold [*P* > 0.05] for *B. thetaiotaomicron* [BT-S1 vs. BT-T1] and 14-fold [*P* < 0.0001] for *B. cellulosilyticus* [BC-S19 vs. BC-S6]; two-way ANOVA, Tukey HSD; *SI Appendix*, Fig. S1*C*).

Growth of strains containing chromosomally targeted gRNAs in liquid LYBHI medium revealed significantly greater delays in the time required to achieve half-maximal density when cultured in aTc-containing vs. unsupplemented medium, compared to control strains containing the scrambled (M1) gRNA (*P* < 0.001; two-way ANOVA, Tukey's HSD; *SI Appendix*, Fig. S1*D*). To examine the genomic correlates of "escape" from lethality, we sequenced the genomes of *B. cellulosilyticus* and *B. thetaiotaomicron* strains that had originally contained a self-targeting gRNA but nonetheless grew to stationary phase in medium containing aTc with or without antibiotic selection (n = 2 strains/ *Bacteroidaceae* species, one with a self-targeting gRNA and the other with the scrambled gRNA [total of 8 cultures/strain]). In the case of *B. cellulosilyticus*, the results revealed a loss of sequencing coverage that encompassed the start of the integrated plasmid through to a 44- to 80-kb region that includes two paralogous serine tRNA genes (*SI Appendix*, Fig. S2*A*). In the case of *B. thetaiotaomicron*, the mechanism was less obvious. Analyzing the results obtained from sequencing *B. thetaiotaomicron* escape isolates disclosed that sequencing coverage of the plasmid region was retained, and surprisingly, coverage was doubled in a distant region flanked by two rRNA gene clusters spanning 300 kb (*SI Appendix*, Fig. S2*B*). Unlike the case of *B. cellulosilyticus*, no loss of coverage across the CRISPR cassette was observed, nor were smaller CRISPR-disrupting

single-nucleotide or insertion/deletion mutants found (as described for a CRISPR kill switch in *E. coli*; ref. 31).

Developing a Model System for In Vivo Knockdown of Targeted *Bacteroides*. Despite the potential for escape, we hypothesized that we could induce a pronounced, albeit transient, in vivo depletion of a knockdown strain from an already established microbial community. To test this hypothesis, we performed a pilot experiment in which adult germfree mice were colonized with a consortium containing 13 cultured, genome-sequenced human gut bacterial strains, including seven *Bacteroidaceae* species. *B. thetaiotaomicron* was represented by the engineered knockdown strain with the *tdk*-targeted BT-T1 gRNA.

The repertoire of glycoside hydrolase and polysaccharide lyase genes represented in the genomes of these community members provides one way of contextualizing their saccharolytic potential. Dataset S1H summarizes the number of GH and PL enzymes in each of the 13 genomes. With a total of 309 GHs and PLs, *B. thetaiotaomicron* ranks third—below *B. ovatus* and *B. cellulosilyticus* which encode 379 and 442 GHs and PLs, respectively, but above the other 10 strains. A heatmap was constructed based on the representation of GHs and PLs families in order to compare the global CAZyme profiles of the 13 community members (*SI Appendix*, Fig. S3). The three strains with the largest number of GHs and PLs clustered together; their clustering appears to be driven by a large expansion of CAZy families GH2 (a multifunctional group of glycoside hydrolases) and GH43 (a family whose members mostly target pectic glycans). Beyond saccharolytic *Bacteroidaceae*, other strains that are members of the CFB (*Cytophaga*, *Fusobacterium*, and *Bacteroides*) group (*O. splanchnicus*), *Firmicutes* (*Ruminococcaceae* sp.), *Actinomycetota* (*C. aerofaciens*), and

Pseudomonadota (*E. coli*) were included in the consortium in the effort to create a simplified gut microbial community with diverse metabolic capabilities. In addition, this community has been shown to reliably and stably colonize gnotobiotic mice, setting the stage for exploring how interbacterial interactions relate to the recognition and utilization of dietary fibers (16, 17, 19).

As shown in *SI Appendix*, Fig. S1*E*, we characterized three groups of mice, each of which consumed the HiSF-LoFV diet supplemented with 10% (w/w) pea fiber (n = 5 animals/arm). They included i) an early treatment group (10 μg/mL aTc [prepared in ethanol] in their drinking water from one day after the gavage of the consortium [day post gavage 1; dpg 1] through dpg 8), ii) a late treatment group (10 μg/mL aTc from dpg 4 to 8) or iii) a control group treated with just the ethanol vehicle (final concentration in drinking water 0.5% v/v; dpg 1 to 8). Fecal samples were collected at 1- to 2-d intervals from each mouse in each group, and the absolute abundance of *B. thetaiotaomicron* was determined by short-read shotgun sequencing of community DNA (32–34). *SI Appendix*, Fig. S1*F* shows that both aTc regimens produced a transient knockdown with a median maximal effect 100-fold for the "early" treatment group and 35-fold for the "late" treatment group compared to vehicle controls (Dataset S2*D*). Based on these results, we selected the late treatment regimen to ensure that community assembly had occurred before inducing targeted knockdown of either *B. cellulosilyticus* or *B. thetaiotaomicron* from the 13-member community.

Effects of Inducible Knockdown on Community Configuration. A 13-member community was introduced into adult germfree C57BL/6J mice: The community contained 12 wild-type strains plus the *B. cellulosilyticus* knockdown strain with BC-S19 gRNA targeting a *susC*-like gene in lieu of its wild-type counterpart. Mice were fed the HiSF-LoFV diet with pea fiber ad libitum and treated with either 10 μg/mL aTc in their drinking water, or the ethanol vehicle alone, from dpg 4 to 8 (n = 10 mice/treatment group) (Fig. 1 *A* and *B*). Five animals in each treatment group were euthanized at dpg 6, while five mice were euthanized at dpg 20. A third arm consisted of mice colonized with an all wild-type, 13-member consortium that received vehicle alone until they were euthanized at dpg 6 (n = 5 mice). Mice from these different treatment groups received a collection of MFABs 4 h prior to their euthanasia so that we could define the saccharolytic activities of their microbial communities. The entire experiment was repeated with modest modifications (the early euthanasia time point was dpg 5 rather than dpg 6, and the duration of the experiment was 12 rather than 20 d (n = 5 to 13 animals/treatment group) (*SI Appendix*, Fig. S4*A*). We measured absolute abundances of consortium members in fecal samples collected beginning on dpg 2 from all mice in both experiments.

In the first experiment, aTc treatment reduced the absolute abundance of *B. cellulosilyticus* by 84 ± 65-fold (mean ± SD) (FDR-corrected *P* < 0.05; linear mixed effects model; Dataset S2*A*). Levels of the organism began to increase from this nadir 2 d after initiation of aTc treatment (dpg 6) and by dpg 20 had attained mean values that were 90.1% (95% CI: 59.2 to 125%) of those documented in animals treated with the ethanol vehicle alone (Fig. 1*B*). Shotgun sequencing of DNA isolated from serially collected fecal samples indicated that on dpg 6 coverage of the *B. cellulosilyticus* knockdown cassette had fallen to 29.9% (95% CI: 24.2 to 35.7%) of that documented in the vehicle control arm (values normalized to the median value for coverage across the entire genome and to the mean coverage in samples procured from mice in the ethanol vehicle–treated control arm). This result suggested that a subpopulation of *B. cellulosilyticus* strains had escaped the kill-switch by deleting the plasmid sequence. Coverage of the region between the site of cassette

integration and one of the organism's two serine tRNA genes (*attB*) located 30 kb downstream fell to 23.6% (95% CI: 17.7 to 29.4%) in dpg 6 fecal samples obtained from mice treated with aTc compared to just ethanol. Similar coverage depths for these regions (cassette and flanking region) were observed in samples collected at dpg 8 (30.3% [95% CI: 18.6 to 42.1%]) and dpg 10 (46.1% [95% CI: 29.4 to 62.9%]) (*SI Appendix*, Fig. S2*C*). The second *B. cellulosilyticus* knockdown experiment using other mice on a separate occasion yielded comparable results. Maximum knockdown (14 ± 9.3-fold, mean ± SD) occurred on dpg 5; knockdown was transient with a subsequent progressive increase in the organism's absolute abundance from dpg 6 to 12 (*SI Appendix*, Fig. S4 *A* and *B* and Dataset S2*B*).

Monosaccharide analysis of cecal contents harvested on dpg 6 disclosed significant reductions in free arabinose, galactose, glucuronic acid, and xylose in aTc-treated compared to vehicle-treated animals (FDR-corrected *P* < 0.05; two-way ANOVA), without a corresponding change in total cecal monosaccharide mass (Dataset S3*A*). As noted above, 5 of the 10 animals in each treatment group were orally gavaged with a collection of MFABs 4 h prior to euthanasia on dpg 6 so that we could define the effect of *B. cellulosilyticus* knockdown on community saccharolytic activity. The input microscopic paramagnetic glass beads were labeled with a fluorophore and were covalently bound to pea fiber arabinan or beechwood xylan via amine groups on the bead surface. These surface amine groups were acetylated in control beads which contained no bound glycans (*Materials and Methods*). Beads were recovered from cecal contents by magnetism, purified by FACS, and the amount of bound glycan quantified by gas chromatography-mass spectrometric (GC-MS) analysis of monosaccharides that had been liberated from the beads by acid hydrolysis. Compared to values obtained from the input preparation of MFABs, there was a statistically significant reduction in the amount of pea fiber arabinan (arabinose) or beechwood xylan (xylose) remaining bound to beads recovered at the nadir of the knockdown and from control groups of mice (*P* < 0.05; one-way ANOVA, Tukey HSD) but no significant differences in the degree of glycan depletion from the MFABs between the aTc- and vehicle-treated animals (*SI Appendix*, Fig. S5 *A* and *B* and Dataset S4*A*). By this criterion, we concluded that the changes produced at the nadir of the knockdown did not compromise the community's capacity to digest pea fiber arabinan (or beechwood xylan).

As noted above, *B. cellulosilyticus* has the largest repertoire of genes encoding carbohydrate-degrading enzymes among the bacteria represented in the consortium: Its genome contains 394 genes encoding glycoside hydrolase modules representing 103 CAZyme families, 30 genes encoding polysaccharide lyases representing 19 CAZyme families, and 94 PULs (2). Applying a linear mixed effects model, we observed that the principal effect of the *B. cellulosilyticus* knockdown on absolute abundances was on two community members, *B. thetaiotaomicron* and *P. vulgatus*. Both these organisms achieved maximum increases 1 to 2 d after the *B. cellulosilyticus* knockdown reached its nadir (FDR-corrected *P* < 0.05; linear mixed effects model; n = 2 independent experiments) (Fig. 1*B*, *SI Appendix*, Fig. S4 *B* and *D*, and Dataset S2 A and B).

Results obtained with an analogous *B. thetaiotaomicron* knockdown experiment provided one way of contextualizing the specificity of the effects of *B. cellulosilyticus* knockdown (Fig. 1*C*). The knockdown nadir in the two independent *B. thetaiotaomicron* experiments was also achieved within 2 d after initiation of aTc administration, (54.9 ± 24.1 and 41.5 ± 22.3-fold reductions [mean ± SD]) and was transient (Fig. 1*C*, *SI Appendix*, Fig. S4 *G–L*, and Dataset S2 E and F). The principal effect of the knockdown was on the abundance of just one community member, *B. finegoldii,* that had not changed

significantly in the *B. cellulosilyticus* knockdown experiment. Although the targeted organism was different, the time course of its effects on other community members was similar: *B. finegoldii* achieved its maximum increase, relative to levels in ethanol-treated controls, 1-2 d after *B. thetaiotaomicron* abundance reached its nadir (FDR-corrected *P* < 0.05; linear mixed effects model; *SI Appendix,* Fig. S4 *I* and *L* and Dataset S2 *E* and *F*).

Effects of Inducible Knockdown of *B. cellulosilyticus* on Expression of Functions by Other Microbial Community Members. We performed microbial RNA-Seq using fecal samples collected at dpg 5 and dpg 6 (1 and 2 d after induction of knockdown) to compare the effects of aTc-treatment vs. ethanol vehicle alone on community gene expression. At each time point, the abundance of transcripts from each organism was modeled using DESeq2 (35) and tested for significant differences in expression (FDR-corrected *P* < 0.05). We annotated the genomes of the 13 community members for their i) CAZymes (2), ii) predicted PULs and CAZyme gene clusters (36), plus iii) inferred metabolic pathways for carbohydrate utilization, fermentation end products, as well as amino acid, and vitamin biosynthesis using the mcSEED platform (37, 38) (Datasets S1G and S5–S7). We subsequently performed gene set enrichment analysis (GAGE; ref. 39) using DESeq2-estimated log$_2$-fold-change to identify PULs or inferred metabolic pathways significantly enriched in the aTc or ethanol treatment groups.

A total of 191 *P. vulgatus* genes were identified as having statistically significant differences in their expression at dpg 5 of the *B. cellulosilyticus* knockdown experiment in aTc-treated vs. ethanol-treated mice; 80 of these genes were components of 20 different PULs plus four "CAZyme gene" clusters (the latter defined as CAZyme-dense regions with no adjacent *susC/D* pair). *P. vulgatus* PUL BVU:1, which has been linked to utilization of xylo-oligosaccharides (XOS), exhibited the greatest increase in expression among *P. vulgatus* PULs (Fig. 2*A* and Dataset S5 *C* and *I*). An orthologous locus expressed in *E. coli* is known to be sufficient for growth on XOS with backbone chain lengths of up six monosaccharide units (40).

B. ovatus differentially expressed 75 genes, 62 of which were associated with PULs and CAZyme gene clusters. PULs Bovatus:26 and Bovatus:81 are both induced with *B. cellulosilyticus* knockdown: Both of these PULs are associated with arabinoxylan and xylan degradation (41) (Fig. 2*B* and Dataset S5 *C* and *G*). This finding supports results from our previous "leave-one-out" experiments that had documented competition between *B. ovatus* and *B. cellulosilyticus* WH2 over arabinoxylan (17). Based on these observations, we assayed the supernatant of *B. ovatus* and *B. cellulosilyticus* in vitro cultures and found that both produce substantial quantities of oligosaccharide fragments when grown on arabinoxylan—findings compatible with utilization of arabinoxylan oligosaccharide fragments by *P. vulgatus*, which induces the PUL BVU:1 upon *B. cellulosilyticus* knockdown (*SI Appendix,* Fig. S6).

B. cellulosilyticus knockdown was also accompanied by statistically significant enrichment in the expression of another *B. ovatus* PUL, Bovatus:52 (FDR-corrected *P* < 0.05; GAGE; Dataset S5A); the first portion of genes within this PUL are involved in galactomannan utilization (Bovatus:52A; refs. 42 and 43). This locus in *B. ovatus* is partially syntenic with a locus in *B. cellulosilyticus* (BcellWH2:27) (Fig. 2*B*). These observations are consistent with the notion that in response to *B. cellulosilyticus* knockdown, *B. ovatus* may prioritize utilization of guar gum and/or other mannan-based thickening agents present in the HiSF-LoFV diet by increasing the expression of Bovatus:52A (Dataset S1E).

B. thetaiotaomicron responded to the *B. cellulosilyticus* knockdown by differentially expressing 131 genes with differential enrichment or depletion of transcripts from 11 predicted PULs on

dpg 5 (compared to ethanol-treated controls). Two PULs associated with pectin utilization, BT:75 (rhamnogalacturonan I, RGI) and BT:13A (rhamnogalacturonan II, RGII) (44, 45), had significant diminution of their expression compared to controls (FDR-corrected *P* < 0.05; GAGE; Dataset S6 A and C). Intriguingly, one day later (dpg 6), expression of BT:75 was enriched to levels that were now significantly greater than those in vehicle-treated controls. While we could not ascertain whether this change reflected alterations in the organism's access to and/or prioritization of RGI as a substrate, we surmised that the pea fiber supplement was a likely source of this RGI given its known glycan composition (19).

Fig. 3 summarizes how these effects of *B. cellulosilyticus* knockdown on gene expression in other community members differ from those documented in the two independent *B. thetaiotaomicron* knockdown experiments. We focused on the fecal microbial community since it could be serially sampled. However, the greater mass of cecal contents obtained from individual animals facilitated MFAB assays of community saccharolytic activity plus mass spectrometric analyses of the levels of monosaccharides and glycosidic linkages. The fact that changes in gene expression within the fecal community paralleled those that occurred within the cecal microbiota (Fig. 3 and Datasets S5 and S6) provided a rationale for integrating results obtained from these two types of biospecimens. As noted above, *B. finegoldii* was the only member of the community that showed statistically significant increases in its absolute abundance with the *B. thetaiotaomicron* knockdown. This change in fitness was accompanied by statistically significant changes in expression of 258 of its genes, including significant increases in expression of genes within PUL BFTSDC17:46 (Dataset S6 A, C, and F). This PUL is partially syntenic to *B. thetaiotaomicron* PUL BT:68, which contains enzymes capable of degrading α-mannosides, raising the question of whether *B. finegoldii* undergoes adaptive foraging of these glycans following *B. thetaiotaomicron* depletion (46). Moreover, in addition to PUL BFTSDC17:46, many of the other PULs in community members that show statistically significant enrichment in expression with *B. thetaiotaomicron* knockdown share i) experimentally determined or predicted polysaccharide substrates with PULs in *B. thetaiotaomicron* (BcellWH2:43 [glycosaminoglycans]; BcellWH2:17 [arabinogalactan]; Bovatus:100 [RGI]) (47) or ii) synteny (BcellWH2:5, Bovatus:12) (see Fig. 3 for predicted substrate specificities and syntenic PULs). Principal component analysis (PCA) was performed on the matrix of mean log$_2$ fold-changes in expression of each PUL in all nontargeted community members for the knockdown experiments shown in Fig. 3. The results revealed separation of the profiles of differential PUL expression (aTc vs. ethanol treatment) in the *B. cellulosilyticus* and *B. thetaiotaomicron* knockdown experiments as well as a split between the dpg 5 and dpg 6 time points for each type of knockdown (*SI Appendix,* Fig S7A).

Together, these results are compatible with the notion that knockdown allows untargeted community members increased access to glycans previously utilized by the depleted knockdown strains. Our analyses focused primarily on carbohydrate utilization between *Bacteroidaceae*. While we observed changes in expression of some metabolic pathways that do not involve carbohydrates in these and other taxa, the most striking changes following knockdown were in metabolic pathways that target just a few carbohydrate species (*SI Appendix, Supporting Information Text* and Datasets S5–S7).

Comparison to Strain Omission Experiments. The *B. cellulosilyticus* knockdown experiments described above included an independent arm where *B. cellulosilyticus* was excluded from the bacterial consortium prior to its gavage and recipient mice were treated with
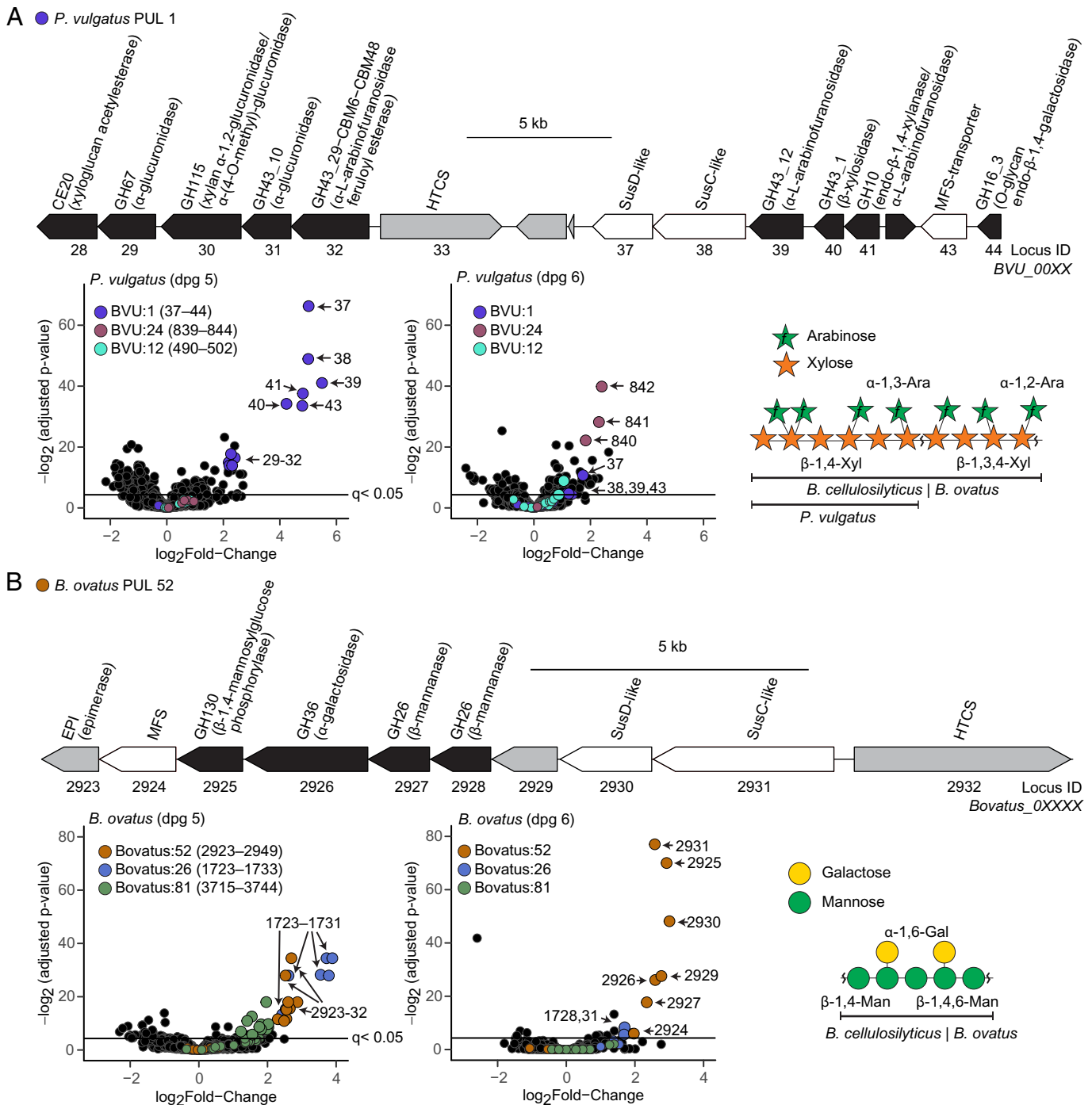
Fig. 2. Effects of *B. cellulosilyticus* knockdown on the expressed functions of *P. vulgatus* and *B. ovatus*. (*A*) Diagram of the *P. vulgatus* oligo-xylan PUL BVU:1 (spanning genes BVU_0028-0044). Differentially expressed *P. vulgatus* transcripts in the fecal communities of mice belonging to the aTc knockdown vs. ethanol vehicle–treated control arms at dpg 5 and 6 (n = 8 and 5 mice, respectively). A model structure of arabinoxylan. Note that *P. vulgatus* can catabolize arabinoxylans with degree of polymerization (DP) up to 6, while *B. cellulosilyticus* and *B. ovatus* are capable of degrading larger polymers (DP greater than 1,000). (*B*) Diagram of the *B. ovatus* galacto/glucomannan PUL Bovatus:52A (encompassing Bovatus_02923-02932). Differentially expressed *B. ovatus* transcripts at dpg 5 and 6 in the fecal microbiota of aTc vs. ethanol vehicle–treated mice (n = 8 and 5, respectively). A model structure of galactomannan, a polysaccharide used by both *B. cellulosilyticus* and *B. ovatus*.

ethanol vehicle (*SI Appendix*, Fig. S7). As with the knockdown experiment, the leave-out community had statistically significant, higher absolute abundances of *P. vulgatus* and *B. thetaiotaomicron* compared to the intact community (n = 5 mice/group; FDR-corrected *P* < 0.05; Welch's *t* test; *SI Appendix*, Fig. S7*B* and Dataset S2 A and B). The PCA described above included the *B. cellulosilyticus* leave-out vs. intact community comparison. The PUL expression profile obtained from this comparison clustered with the profile obtained from the dpg 5 aTc vs. ethanol comparison

in the knockdown experiment (*SI Appendix*, Fig. S7*A*). Significant differences in the expression of xylan loci in *P. vulgatus* (and *B. ovatus*) documented in the knockdown experiment paralleled those documented in the comparison of the 12-member leave-out and 13-member ("non-leave-out") control (*SI Appendix*, Fig. S7 *C* and *D*). Interestingly, no difference in the abundance of *B. ovatus* galactomannan locus transcripts was observed in the leave-out comparison (*SI Appendix*, Fig. S7*D*), providing one piece of evidence that a microbial community's "history" (i.e., depleting
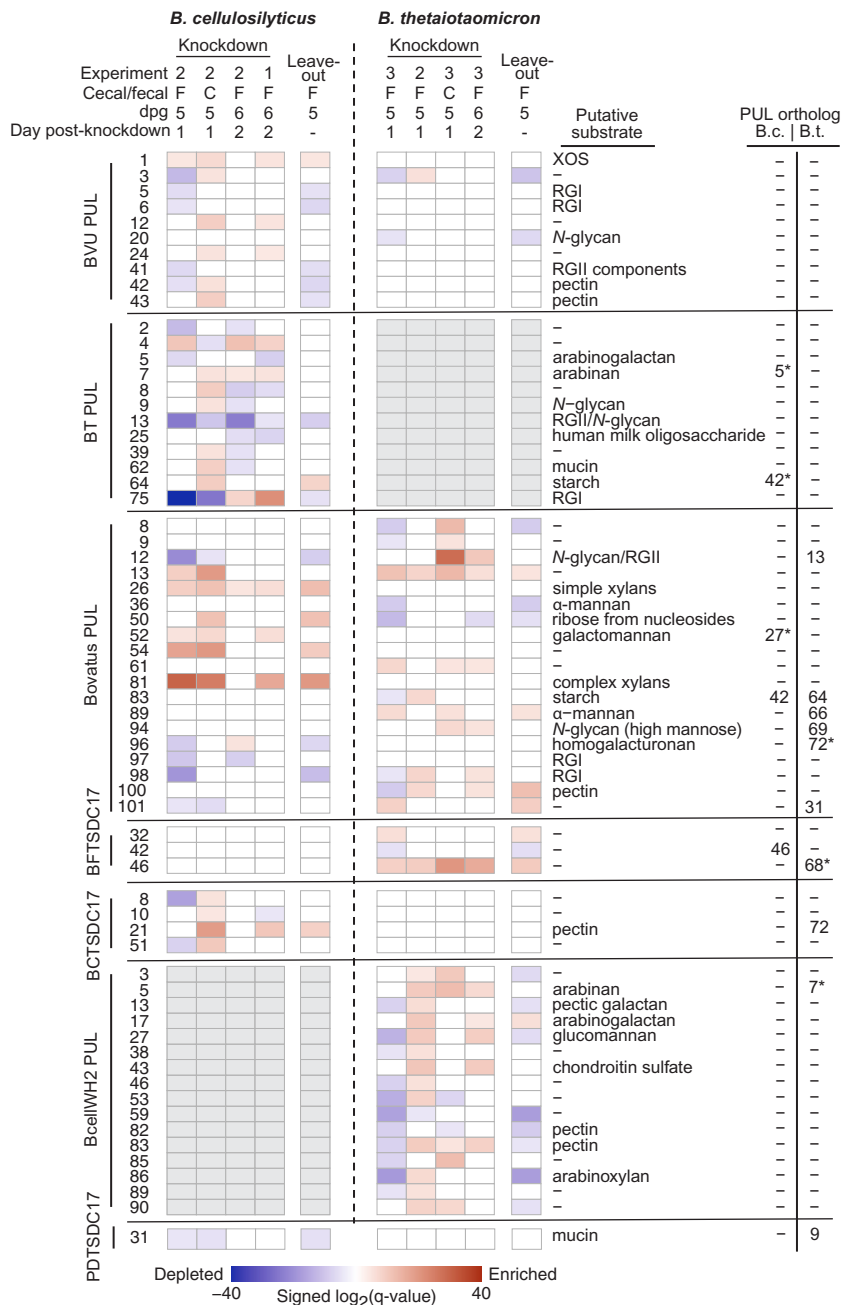
Fig. 3. Effects of *B. cellulosilyticus* and *B. thetaiotaomicron* knockdown and "leave-out" on expression of PULs in other community members. PULs from *B. cellulosilyticus* and *B. thetaiotaomicron* knockdown (aTc-treated vs. vehicle-control) and leave-out experiments (leave-out vs. complete community) are shown. On dpg 4, groups of animals in the knockdown experiment received aTc or ethanol vehicle while animals in the leave-out experiment just received ethanol vehicle. Color scale corresponds to −Sign(change) × log₂(FDR-corrected *P* value) generated by GAGE (Generally Applicable Gene set Enrichment). Positive values indicate enrichment in aTc-treated or leave-out condition. Cells corresponding to PULs with nonsignificant enrichment (FDR-corrected *P* value > 0.05) are colored white. PUL "orthologs" were defined by the PUL database (PUL-DB) PUL aligner tool (36, 48) with inexact or partial matches marked by an asterisk. Putative substrates for each PUL are based on literature reports of biochemical studies or by sequence/domain similarity to characterized enzymes/PULs (Datasets S5 and S6).

B. cellulosilyticus after colonization vs. no history of *B. cellulosilyticus* exposure) affects its metabolic state (49).

Motivated by these results, we designed a set of experiments to further disentangle the mechanisms that underlie the metabolic competition between *P. vulgatus* and *B. cellulosilyticus*. To do so, we used a genetic approach based on CRISPR base editing.

Applying Cytidine Deaminase Mutagenesis to Further Examine the Response of *P. vulgatus* to *B. cellulosilyticus* Knockdown. We hypothesized that abrogating the function of the XOS utilization pathway in *P. vulgatus* (PUL BVU:1) might inhibit its expansion after *B. cellulosilyticus* knockdown while leaving its basal fitness unchanged. Conversely, we postulated that disrupting its capacity for arabinan utilization would result in an overall loss of fitness, since we had previously shown that expression of the *P. vulgatus* arabinan PUL, BVU:27 is increased significantly in mice fed the pea fiber–supplemented HiSF-LoFV diet compared to those fed the corresponding unsupplemented diet (17, 19). To test these

hypotheses, we leveraged our genetic tools and applied a system for CRISPR base editing to *Bacteroidaceae*. This system consists of an aTc-inducible dCas9-PmCDA1 gene and a constitutively expressed guide RNA. When the complex is bound, the PmCDA1 domain can deaminate cytosine bases within a 15 to 20 bp window 5′ of the protospacer adjacent motif (PAM) site (50, 51). The deaminated cytosine (uracil) is "read" during DNA replication as a thymine, resulting in a C→T transition.

We incorporated this system into the pNBU2 integration vector (pNBU2_CDA) as well as into a stably expressed plasmid (pMob_CDA) (Fig. 4A). After inducing mutations with the pMob vector, we found that strains could be cured of the plasmid within 1-4 passages on LYBHI medium without selection, at which point no cultures tested had Erm-resistant growth, and the strains contained mutations induced by cytidine deaminase within the predicted site that was complementary to each gRNA. To determine the efficiency of mutagenesis produced by this two-step aTc induction of Cas9-guided cytidine deamination, we targeted loci in *P. vulgatus*
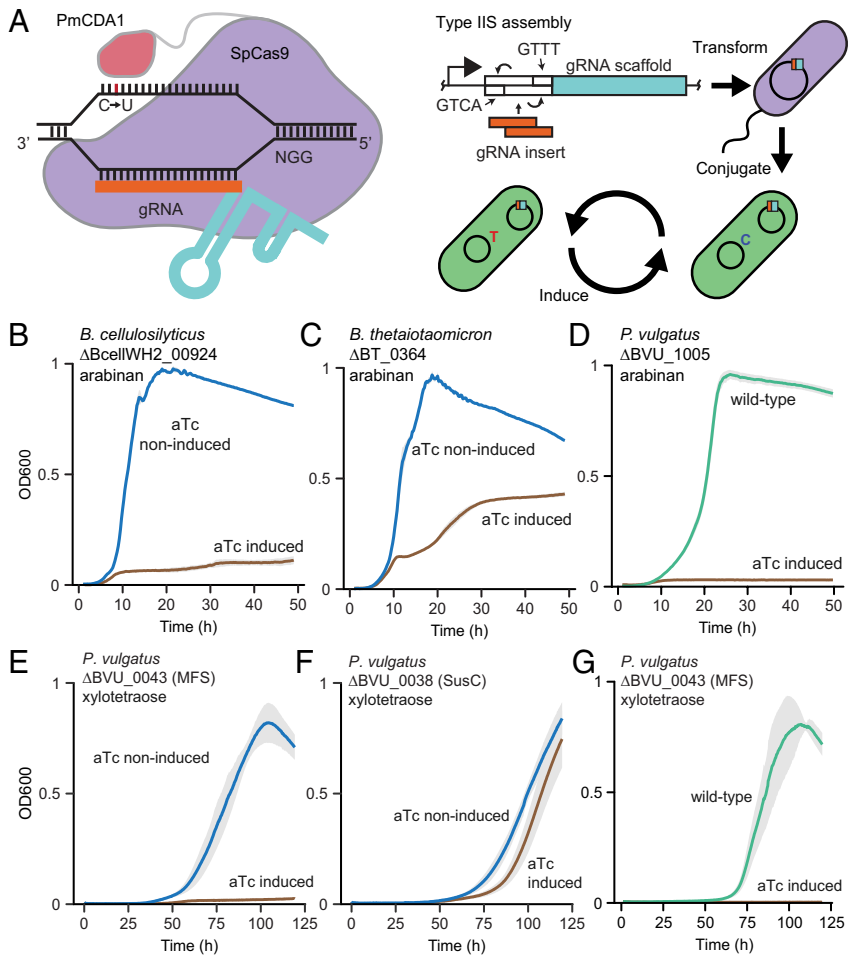
Fig. 4. Cytidine deaminase mutagenesis tests of the necessity of selected PUL-associated carbohydrate transporters for in vitro growth of *B. cellulosilyticus*, *P. vulgatus*, and *B. thetaiotaomicron*. (*A, Left*) Diagram of cytidine deaminase mutagenesis workflow applied to *Bacteroidaceae*. SpCas9-PmCDA1 protein complexes with a gRNA and DNA to deaminate cytosine to uracil, which is then read as thymine by DNA polymerase during DNA replication. (*Right*) Strains containing a construct for cytidine deaminase mutagenesis were generated by i) type IIS assembly of parent pMob or pNBU2 vectors containing gRNA inserts, ii) transformation of one of the constructs into competent *E. coli* cells, and iii) conjugation of these cells with recipient *Bacteroidaceae*. The resulting strains were subsequently induced to express SpCas9-PmCDA1 by exposing them to aTc. (*B–G*) Growth of the indicated bacterial strains in *Bacteroides* Minimal Medium (BMM) supplemented with the indicated carbon sources. The shaded region encompasses the 95% LOESS CI (n = 3 replicate cultures per condition). *P. vulgatus* ΔBVU_0043 (MFS transporter in the oligo-xylan PUL) and ΔBVU_1005 (SusC-transporter in the arabinan PUL) are denoted as ΔXOS and ΔAbn, respectively, in Fig. 5 and Dataset S7.

(BVU_0038, BVU_0043, BVU_1005) and *B. thetaiotaomicron* (BT_0362, BT_0364) using vector backbones pMob and/or pNBU2. Isolates were subjected to amplicon sequencing to estimate the rate of cytidine conversion. Noninduced isolates (n = 3) were compared to isolates derived from cultures that had undergone one or two rounds of aTc induction (*Materials and Methods*). After the first induction cycle, 36% of reads collected from induced isolates possessed the desired mutant allele (range: 3 to 66%), while after two cycles, an average of 52% of reads possessed the desired allele (range: 13 to 92%) (*SI Appendix*, Fig. S8*A*).

Using type IIS restriction enzyme assembly to insert a gRNA sequence, pNBU2_CDA or pMob_CDA vectors were constructed, transformed, and conjugated into three target *Bacteroidaceae* species; the resulting strains were grown in liquid medium supplemented with aTc and then plated on aTc-supplemented agar. This approach allowed us to introduce stop codons into the *susC*-homolog within the arabinan PULs that are syntenic and conserved across *B. cellulosilyticus* (PUL BcellWH2:5, BcellWH2_00924), *B. thetaiotaomicron* (PUL BT:7, BT_0364), and *P. vulgatus* (PUL BVU:27, BVU_1005).

In all organisms, growth of stop codon mutants was severely limited on BMM containing sugar beet arabinan, compared to noninduced pNBU2_CDA integrants or wild-type controls for nonintegrated mutants (Fig. 4 *B–D*). Disruption of the major facilitator superfamily (MFS) gene in *P. vulgatus* PUL BVU:1 (BVU_0043, Q157*) resulted in a loss of growth on BMM containing xylotetraose (Fig. 4 *E* and *G*). Conversely, disrupting the SusC-like transporter BVU_0038 (W456*) located in PUL BVU:1 had minimal effects on growth in BMM containing

xylotetraose (Fig. 4*F*). These findings suggest that the MFS transporter is responsible for import of xylotetraose or its degradation products. We obtained similar findings for these strains using other oligo-xylan species (e.g., those with degree of polymerization of 2 to 6). Growth on beechwood xylan was abrogated or severely delayed by both mutants (*SI Appendix*, Fig. S8*B*).

We subsequently performed a *B. cellulosilyticus* knockdown experiment in three different 13-member community contexts: one where *P. vulgatus* was wild-type (WT); one where it had a BVU_0043 disruption (Q157*); and another where the strain contained a BVU_1005 disruption (Q256*) (abbreviated in Fig. 5 as ΔXOS and ΔAbn, respectively). Mice harboring each of these communities were treated with aTc or ethanol-vehicle control (n = 5/treatment/community type) beginning on dpg 4 and then euthanized on dpg 12 (Fig. 5*A*). The absolute abundances of the ΔAbn and ΔXOS mutants in feces were not significantly different from wild-type *P. vulgatus* across the ethanol-control arms (P > 0.05; linear mixed effects model, Tukey HSD; Fig. 5*B* and Dataset S2C). However, at the point of maximal *P. vulgatus* increase in the aTc treatment arm (dpg 7), the absolute abundance of wild-type *P. vulgatus* increased more than the ΔAbn strain (12.51 ± 2.98 vs. $4.61 \pm 1.46 \ 10^6$ genomes/mg feces; P < 0.05; linear mixed effects model), suggesting that arabinan utilization becomes a fitness determinant for (wild-type) *P. vulgatus* during *B. cellulosilyticus* knockdown (Fig. 5*B*). Despite the strong correlation between increased expression of XOS-utilization genes in PUL BVU:1 and the increased fitness of *P. vulgatus* during *B. cellulosilyticus* knockdown, genetically disrupting this pathway in *P. vulgatus* had no significant impact on its absolute abundance
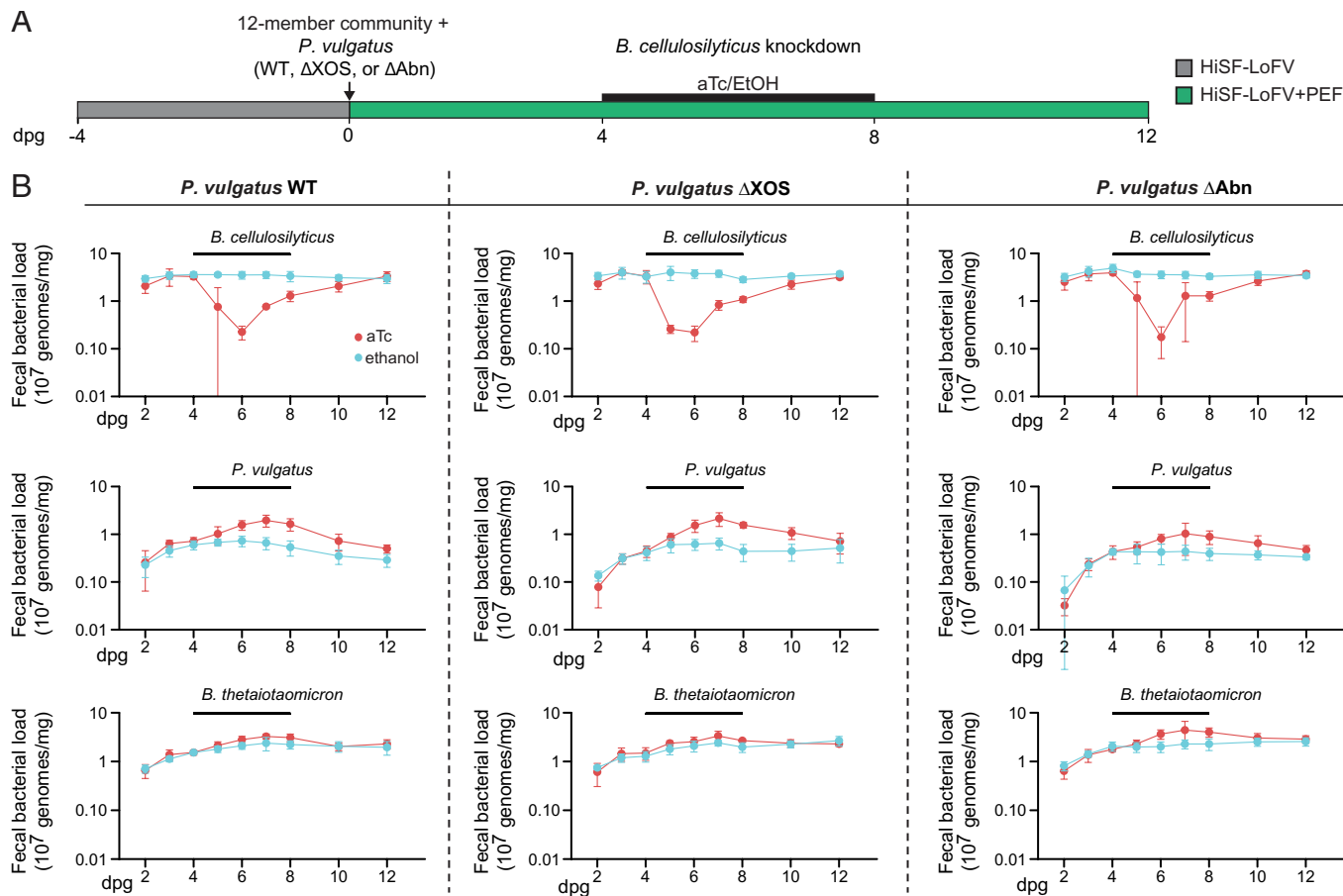
Fig. 5. *B. cellulosilyticus* knockdown effects on genetically manipulated *P. vulgatus* strains. (*A*) Experimental design. Germfree mice were fed HiSF-LoFV diet for 4 d prior to colonization and then colonized with a 13-member gut bacterial consortium. *B. cellulosilyticus* was represented by the inducible knockdown mutant (BC-S19). *P. vulgatus* was represented by the wild-type strain or a plasmid-cured cytidine deaminase mutant strain (ΔXOS [BVU_0043 disruption (Q157*)] or ΔAbn [BVU_1005 disruption (Q256*)]). After oral gavage, mice were fed HiSF-LoFV+10% PEF (w/w) and treated with aTc or ethanol vehicle in their drinking water from dpg 4-8. Mice were euthanized on dpg 12. (*B*) Absolute abundance of the indicated organisms in the experimental arms that included the wild-type, ΔXOS, or ΔAbn strains of *P. vulgatus*. Mean values ± SD are plotted on a logarithmic scale (see Dataset S2C for raw values) (n = 5 mice/group).

($P > 0.05$; linear mixed effects model; Fig. 5*B*). As alluded to in the *Introduction* section and discussed below, these findings support a strategy for glycan prioritization based on coutilization, rather than sequential utilization which has been posited as a mechanism for coexistence of members of a saccharolytic microbial community (8, 9).

Transcriptional responses to *B. cellulosilyticus* Knockdown in Communities Containing Wild-Type and Mutant *P. vulgatus* Strains. The effects of *B. cellulosilyticus* knockdown on community gene expression were characterized over time. We first compared aTc-treated animals with their vehicle-treated controls at days postgavage (dpg) 4 through 8, 10, and 12, focusing on mice harboring the community with the wild-type *P. vulgatus* strain (n = 5 animals). In this community context, 28 PULs in five *Bacteroidaceae* exhibited statistically significant differences in their expression after initiation of *B. cellulosilyticus* knockdown on dpg 5, 6, or 8 (FDR-corrected $P < 0.05$; GAGE; Dataset S7). Twenty five percent of the differentially expressed PULs manifested their maximal differential expression 1 d after initiating knockdown at dpg 5. For example, the *P. vulgatus* PUL involved in oligo-xylan metabolism (BVU:1), and each of *B. ovatus*' two xylan utilization PULs (Bovatus:26 and Bovatus:81) was expressed at significantly higher levels in aTc-treated animals compared to ethanol controls at dpg 5. The expression levels of these three xylan PULs returned to those documented in ethanol

controls by dpg 7 (*SI Appendix*, Fig. S9 *A and B* and Dataset S7 *G and I*). In contrast, genes in the *B. ovatus* galactomannan PUL, Bovatus:52A, achieved maximal differential expression at dpg 6 and remained at higher levels until dpg 8-9, which may reflect a relatively longer-lasting galactomannan "niche" (*SI Appendix*, Fig. S9*C* and Dataset S7G). The xylose utilization genes (*xylRBAE*) in *B.ovatus* demonstrated the same pattern of increased expression during dpg 5-6. By dpg 10, only one PUL (Bovatus:13) was differentially enriched in the aTc treatment arm (GAGE); i.e., its level of expression remained significantly higher compared to the ethanol controls, while the other 27 formerly differentially expressed PULs in the five *Bacteroidaceae* exhibited levels that were not significantly different from those in the control group (Dataset S7G).

We performed parallel gene expression analyses of the communities containing the *P. vulgatus* ΔXOS and ΔAbn mutants, comparing aTc-treated animals to vehicle control animals at dpg 4-6, 8, and 10. In both of these communities, differentially expressed genes in the *P. vulgatus* mutant strains and in *B. ovatus* at dpg 5 and 6 had significant overlap with the *P. vulgatus* WT comparison ($P < 5 \times 10^{-10}$; chi-squared test). Overall, we identified transcripts from up to 75 PULs in the community's *Bacteroidaceae* that were significantly enriched after initiation of *B. cellulosilyticus* knockdown in the communities containing the *P. vulgatus* ΔXOS and ΔAbn mutants (FDR-corrected $P < 0.05$; GAGE; Dataset S7); notably, this pattern of differential PUL expression was similar to

that observed in the community harboring the wild-type *P. vulgatus*. For example, transcripts from xylan utilization PULs (BVU:1, Bovatus:26, and Bovatus:81) and the *B. ovatus* galactomannan PUL (Bovatus:52A) were present at significantly higher levels in aTc-treated animals vs. vehicle controls at dpg 5 and/or 6 in each community containing one of the three *P. vulgatus* strains.

Overall, these findings suggest that while our genetic manipulations of *P. vulgatus* reduced its fitness in response to *B. cellulosilyticus* knockdown, carbohydrate utilization in other community members was minimally affected, underscoring the resiliency and robustness of the community's saccharolytic activities.

Discussion

Understanding how members of the human gut microbiota prioritize nutrient resources represents one important step in deciphering the mechanisms that determine community robustness and resiliency in health and in various disease states. Obtaining this knowledge is foundational for developing microbiota-directed therapeutics. Here, we generated inducible CRISPR mutants for knockdown of *B. cellulosilyticus* or *B. thetaiotaomicron* from a 13-member consortium of cultured human gut bacteria established in gnotobiotic mice monotonously fed a representative Western (USA) diet high in saturated fat diets, low in fruits and vegetables but supplemented with pea fiber. This defined community contained a total of 7 different *Bacteroidaceae* species. Replicated knockdown experiments demonstrated that the decrease in absolute abundance of *B. cellulosilyticus* or *B. thetaiotaomicron* was rapid, reaching a nadir within 1 to 2 d; knockdown was accompanied by reproducible changes in the absolute abundances of other community members and shifts in expression of polysaccharide utilization loci (PULs) across the community. While expression changes were evident as early as one day after knockdown, shifts in the abundances of other community members lagged behind the maximum knockdown effect by another 1 to 3 d, illustrating that the kinetics of community compositional changes are relatively slow in this model system.

At the community level, functional redundancy in saccharolytic activity following each knockdown was demonstrated by measuring levels of glycans remaining on the surfaces of microscopic "artificial food particles" that had been orally administered and then retrieved from the intestines of gnotobiotic mice, and by mass spectrometry of glycosidic linkages present in intestinal contents. We attempted to disturb this functional redundancy in a single community member by genetically disabling the function of an oligo-xylan PUL in *P. vulgatus* —the organism that exhibited the greatest abundance increase in response to *B. cellulosilyticus* knockdown. Genetic manipulation of this PUL limited its growth in vitro on defined (oligo-) xylan carbon sources but did not have a measurable effect on *P. vulgatus* fitness in vivo. In general, our results are consistent with a scheme of coutilization of nutrient resources by *P. vulgatus* or at least coexpression of its PULs targeting oligo-xylans and arabinans in this community and diet context, rather than a scheme of sequential and hierarchical PUL expression and utilization of different available glycans (8, 9). "Fast-switching" between nutrient resources and coutilization of resources can be viewed as part of a continuum. "Faster-switching" could be a competitive advantage for *P. vulgatus* over other "slow-switching" strains in a rapidly changing resource environment (10, 52, 53) but may come at fitness cost in a more static resource environment. These strategies for regulating nutrient utilization may also contribute to priority effects observed during colonization of the gut and other habitats (54). These and other mechanisms underlying priority effects could be delineated by knockdown experiments of the type described in this report and by knockdown experiments where the community is also challenged by an "invading" organism.

In conclusion, the approach of inducing CRISPR knockdowns of a given target organism provides an opportunity to refine models of interbacterial interactions in the gut microbiota. By observing changes in the expressed functions of untargeted members following knockdown, we can observe the imprint/effects of the depleted strain on other community components. In principle, experiments can be designed where defined communities contain multiple wild-type strains of a given species (or stop-codon mutant pools derived from a given parental strain). This latter feature offers an opportunity to knock down one species and dissect the strain-level determinants of another species' response. This capacity, coupled with prebiotic screens, offers an opportunity to further understand the significance of strain level diversity in the human gut microbiota in a broader dimension and to facilitate development of prebiotic, probiotic, and symbiotic therapeutics. Moreover, extensions and modifications of this experimental paradigm could examine the determinants of priority effects and of community assembly that are currently poorly understood.

Limitations of the Current Study. The inducible knockdown system described here does not result in extirpation of the CRISPR target organism from the community. We regard this as a desirable feature as it resembles the response of the human gut microbiota to many "real-world" perturbations where members dynamically change their abundance and expressed functions following transient or periodic events (e.g., changes in diet, exposure to drugs, invasion by enteropathogens, etc.). As such, escape (recovery) from knockdown provides an opportunity to characterize the kinetics of perturbation and re-equilibration and coincidently gain insights about mechanisms that underlie community resiliency and robustness. While many responses were apparent by comparisons of mean effects at the nadir of the knockdown, the system should be used for more detailed kinetic modeling of interbacterial interactions during recovery. Although more work needs to be done to elucidate the genomic correlates of escape from the CRISPR knockdown, it is unclear at present how much we will be able to control the duration of the knockdown. Refining the knockdown system could include i) using multiple integration sites to avoid cassette deletion or disruption, ii) refining Cas9 expression via optimized promoters, degrons, or induction switches to reduce any noninduced "leaky" Cas9 protein expression that might lead to premature escape, and iii) adding redundant effector mechanisms (e.g., self-targeting type VI secretion systems or toxin/anti-toxin proteins) may increase knockdown efficiency and duration (30, 31, 55). Furthermore, adding prebiotic interventions, based on knowledge of adaptive nutrient utilization strategies documented in initial knockdown experiments, could be a means for testing ways to facilitate sustained adaptations to a knockdown (perturbation). In its current form, the cytidine deaminase mutagenesis protocol has limited efficiency and is dependent on positive selection. To improve efficiency, future iterations could include refined guide RNA targeting and/or covalently linking uracil glycosylase inhibitor domains to the SpCas9 complex. Finally, more work is needed to interpret the results of experiments of this type, including the need to further characterize the network of PUL regulation across species/strains of *Bacteroidota* in communities of different composition and complexity under various defined dietary conditions.

Materials and Methods

Generation of Plasmids. Plasmids were constructed by Gibson cloning (NEBuilder® HiFi DNA Assembly Master Mix, New England BioLabs [NEB]). pNBU2-based plasmids (pNBU2-CRISPR, pNBU2-CDA) were constructed using the pExchange-tdk plasmid backbone (RP4-oriT, R6K ori, *bla*, *ermG*) and NBU2 integrase from pNBU2-tetQb. pMobA.repA-CDA (aka pMob_CDA) was

constructed using the pLYL01 plasmid backbone (pBR322, *bla*, *mobA*, *repA*, *ermF*). All plasmids were generated with anhydrotetracycline (aTc)-inducible CRISPR cassettes (P2-A21-tetR, P1TDP-GH023-SpCas9 or P1TDP-GH023-dSpCas9-PmCDA1, P1-N20 sgRNA scaffold) that were assembled from synthetic double-stranded oligonucleotides and a PCR amplicon from *Streptococcus pyogenes* strain SF370 genomic DNA. To generate cefoxitin-resistant plasmids, the erythromycin (*ermG*) antibiotic resistance gene was replaced by the cefoxitin antibiotic resistance gene (*cfxA*) using synthetic DNA and traditional restriction enzyme cloning. Inactivating Cas9 mutations (D10A and H840A) were introduced by site-directed mutagenesis followed by plasmid amplification (Q5 High-Fidelity DNA polymerase, NEB), plasmid amplification, parental plasmid strand digestion (DpnI, NEB), and bacterial transformation.

To generate cytidine deaminase mutants, spacer sequences were designed using CRISPRseek (56) and custom R scripts to filter for sequences with a high Doench_2014 score that could introduce a stop codon in the first half of the target gene. Oligonucleotides (obtained from IDT) of the spacer sequence with sticky ends (CAGT-spacer, RC spacer-AAAC) were annealed and phosphorylated (T4 kinase, NEB). The annealed oligos and 50 ng of parental vector (pNBU2_CDA or pMob_CDA) were combined at a molar ratio of 3:1 and treated with AarI (ThermoFisher) and T4 ligase (NEB) at 37 °C for 1 h. For transformation, a 4 μL aliquot of this reaction mixture was added to 20 μL of chemically competent S17 cells (57) or by electroporation of a mixture composed of 1 μL aliquot of the reaction mixture plus f 24 μL of electrocompetent S17 cells (NEB electroporation protocol C2986). Transformed cells were selected on LB medium containing 50 μg/mL carbenicillin and subsequently conjugated with *Bacteroidaceae* using a previously reported method (58). Conjugated *Bacteroidaceae* were selected on BHI medium containing 10% horse blood, 200 μg/mL gentamycin, and 25 μg/mL erythromycin or 20 μg/mL cefoxitin. Induction of mutation was executed using overnight growth in LYBHI medium containing 200 ng/mL aTc with subsequent plating on BHI medium plus 10% horse blood and 200 ng/mL aTc (erythromycin was added for plasmid inductions).

Cytidine-Deaminase Mutant Validation. To assay the efficiency of mutagenesis, three colonies were examined for each of the uninduced species. Cultures of one of the three colonies were then induced with aTc, with 10 colonies from this first round of induction collected from the plating. Cultures of five of the 10 underwent a second round of aTc induction. Three colonies collected from each of the subcultures from this last round were subjected for sequencing of PCR amplicons generated from the genomic targets.

Mutations were confirmed by amplicon sequencing with the nested PCR priming scheme (Illumina document #1000000002694 v10). To do so, the target region was first amplified using NEB HotStart Q5 for 25 cycles. Next, 5 μL of the reaction was amplified for 10 cycles with primers that attached Illumina Nextera indices using NEB HotStart Q5. Finally, these amplicons were pooled, purified using Ampure bead selection, and sequenced on an Illumina MiSeq or NextSeq instrument to generate 2x250 nucleotide reads. Reads were aligned to bacterial genomes using BWA-mem (v 0.7.17-r1188; ref. 59). These alignments were then processed (bcftools, v1.12, ref. 60) to generate pile-up statistics across the aligned bases. Mutagenesis efficiency was reported as the fraction reads with the desired allele at each position within the window of predicted cytidine deaminase activity.

Gnotobiotic Mouse Husbandry. Gnotobiotic mouse experiments were performed using protocols approved by the Washington University Animal Studies Committee. Germfree male C57BL/6J mice were housed in plastic flexible film isolators (Class Biologically Clean Ltd) at 23 °C under a strict 12-h light cycle (lights on at 0600h). Mice were maintained on an autoclavable mouse chow (Envigo; Cat. No. 2018S). Cages contained paper houses for environmental enrichment and autoclaved bedding (Aspen Woodchips; Northeastern Products).

The HiSF-LoFV experimental diet was produced using human foods (Dataset S1E), approximating the lowest tertile of fruits and vegetable intake and the highest tertile of saturated fat intake as reported by the National Health and Nutrition Examination Survey (NHANES) database (15). The diet was milled to powder (D90 particle size, 980 mm) and mixed with 10% (w/w) pea fiber (Rattenmaier; Cat. No. Pea Fiber EF 100). The milled diet ± pea fiber mixture was then extruded into pellets. Pellets were packaged, vacuum sealed, and sterilized by gamma irradiation (20-50 kilograys, Steris, Mentor, OH). Sterility was confirmed by culturing the diet in TYG medium under aerobic and anaerobic conditions (atmosphere: 75% N_2, 20% CO_2, 5% H_2) at 37 °C and by short-read shotgun sequencing of fecal DNA prepared from germfree mice consuming the pelleted HiSF-LoFV diet.

Stock solutions of anhydrotetracycline hydrochloride (37919, Millipore Sigma) were generated (2 mg/mL in ethanol) and filter-sterilized (Millipore Sigma SLGV033RS filters). Drinking water containing aTc (10 μg/mL 0.5% ethanol) or 0.5% ethanol alone was prepared daily or every other day (experiment shown in *SI Appendix*, Fig. S1 *E, F*) in gnotobiotic isolators.

Mice were fed a HiSF-LoFV diet for 4 d prior to colonization. After colonization, mice were singly housed and received the HiSF-LoFV diet ± 10% pea fiber. During treatment periods (Fig. 1), drinking water supplemented with aTc or ethanol vehicle was substituted. aTc or ethanol treatment was initiated at dpg 4 for all experiments shown except for the experiment described in *SI Appendix*, Fig. S1 *E and F*. This four-day "delay" was designed to help ensure that the community had assembled in a consistent manner across animals prior to initiating the targeted knockdown. At the end of the treatment period, aTc was withdrawn and bedding was replaced. Fresh fecal samples were collected in 1.8-mL screw-top plastic vials (Axygen) from each animal within seconds of being produced.

See *SI Appendix, Methods* for descriptions of procedures for i) bacterial culture, ii) bacterial genome sequencing, iii) MALDI-TOF MS of oligosaccharides in bacterial cultures, iv) determination of absolute abundances of consortium members in gnotobiotic mice using short-read sequencing of community DNA; v) escape mutant analysis, vi) microbial RNA-Seq, vii) MFAB analysis of community saccharolytic activity, and viii) mass spectrometric analysis of cecal monosaccharides and glycosidic linkages.

Author affiliations: ᵃEdison Family Center for Genome Sciences and Systems Biology, Washington University School of Medicine, St. Louis, MO 63110; ᵇCenter for Gut Microbiome and Nutrition Research, Washington University School of Medicine, St. Louis, MO 63110; ᶜGenome Engineering R&D, MilliporeSigma, the Life Science business Merck KGaA, Darmstadt, Germany, St. Louis, MO 63103; ᵈArchitecture et Fonction des Macromolécules Biologiques, Centre National de la Recherche Scientique and Aix-Marseille University, 13288 Marseille, France; ᵉDepartment of Biotechnology and Biomedicine, Technical University of Denmark, Kgs. Lyngby DK-2800, Denmark; ᶠDepartment of Biological Sciences, King Abdulaziz University, Jeddah 21589, Saudi Arabia; ᵍInfectious and Inflammatory Disease Center, Sanford Burnham Prebys Medical Discovery Institute, La Jolla, CA 92037; and ʰDepartment of Chemistry, University of California, Davis, CA 95616

Author contributions: Z.W.B. and J.I.G. designed research; Z.W.B., D.A.W., T.R.S., J.L.G., A.E.B., C.S., N.P.B., Y.C., G.C., Z.Z., C.H.M., and E.R.E. performed research; Z.W.B., T.R.S., Z.Z., and E.R.E. contributed new reagents/analytic tools; Z.W.B., D.A.W., T.R.S., S.H., N.T., B.H., D.A.R., A.L.O., C.B.L., E.R.E., G.D.D., and J.I.G. analyzed data; and Z.W.B. and J.I.G. wrote the paper.

Reviewers: L.C., University of Chicago; and G.D.W., University of Pennsylvania.

1. A. El Kaoutari, F. Armougom, J. I. Gordon, D. Raoult, B. Henrissat, The abundance and variety of carbohydrate-active enzymes in the human gut microbiota. *Nat. Rev. Microbiol.* **11**, 497–504 (2013).
2. E. Drula *et al.*, The carbohydrate-active enzyme database: functions and literature. *Nucleic Acids Res.* **50**, D571–D577 (2022).
3. J. M. Grondin, K. Tamura, G. Déjean, D. W. Abbott, H. Brumer, Polysaccharide utilization loci: Fueling microbial communities. *J. Bacteriol.* **199**, e00860-16 (2017).
4. P. Lapébie, V. Lombard, E. Drula, N. Terrapon, B. Henrissat, *Bacteroidetes* use thousands of enzyme combinations to break down glycans. *Nat. Commun.* **10**, 2043 (2019).
5. N. A. Pudlo *et al.*, Phenotypic and genomic diversification in complex carbohydrate-degrading human gut bacteria. *mSystems* **7**, e0094721 (2022).
6. G. Hardin, The competitive exclusion principle: An idea that took a century to be born has implications in ecology, economics, and genetics. *Science* **131**, 1292–1297 (1960).
7. J. Monod, The growth of bacterial cultures. *Annu. Rev. Microbiol.* **3**, 371–394 (1949).
8. N. D. Schwalm III, G. E. Townsend, E. A. Groisman, Prioritization of polysaccharide utilization and control of regulator activation in *Bacteroides thetaiotaomicron*. *Mol. Microbiol.* **104**, 32–45 (2017).
9. Y. E. Tuncil *et al.*, Reciprocal prioritization to dietary glycans by gut bacteria in a competitive environment promotes stable coexistence. *mBio* **8**, e01068-17 (2017).
10. B. Bloxham, H. Lee, J. Gore, Diauxic lags explain unexpected coexistence in multi-resource environments. *Mol. Syst. Biol.* **18**, e10630 (2022).
11. S. Rakoff-Nahoum, M. J. Coyne, L. E. Comstock, An ecological network of polysaccharide utilization among human intestinal symbionts. *Curr. Biol.* **24**, 40–49 (2014).
12. S. Rakoff-Nahoum, K. R. Foster, L. E. Comstock, The evolution of cooperation within the gut microbiota. *Nature* **533**, 255–259 (2016).
13. O. Delannoy-Bruno *et al.*, Evaluating microbiome-directed fibre snacks in gnotobiotic mice and humans. *Nature* **595**, 91–95 (2021).
14. O. Delannoy-Bruno *et al.*, An approach for evaluating the effects of dietary fiber polysaccharides on the human gut microbiome and plasma proteome. *Proc. Natl. Acad. Sci. U.S.A.* **119**, e2123411119 (2022).
15. V. K. Ridaura *et al.*, Gut microbiota from twins discordant for obesity modulate metabolism in mice. *Science* **341**, 1241214 (2013).
16. M. Wu *et al.*, Genetic determinants of in vivo fitness and diet responsiveness in multiple human gut *Bacteroides*. *Science* **350**, aac5992 (2015).
17. M. L. Patnode *et al.*, Interspecies competition impacts targeted manipulation of human gut bacteria by fiber-derived glycans. *Cell* **179**, 59–73 (2019).
18. M. L. Patnode *et al.*, Strain-level functional variation in the human gut microbiota based on bacterial binding to artificial food particles. *Cell Host Microbe* **29**, 664–673 (2021).
19. D. A. Wesener *et al.*, Microbiota functional activity biosensors for characterizing nutrient metabolism in vivo. *ELife* **10**, e64478 (2021).
20. A. Reyes, M. Wu, N. P. McNulty, F. L. Rohwer, J. I. Gordon, Gnotobiotic mouse model of phage–bacterial host dynamics in the human gut. *Proc. Natl. Acad. Sci. U. S. A.* **110**, 20236–20241 (2013).
21. B. B. Hsu *et al.*, Dynamic modulation of the gut microbiota and metabolome by bacteriophages in a mouse model. *Cell Host Microbe* **25**, 803–814 (2019).
22. M. R. O'Connell *et al.*, Programmable RNA recognition and cleavage by CRISPR/Cas9. *Nature* **516**, 263–266 (2014).
23. A. C. Komor, Y. B. Kim, M. S. Packer, J. A. Zuris, D. R. Liu, Programmable editing of a target base in genomic DNA without double-stranded DNA cleavage. *Nature* **533**, 420–424 (2016).
24. K. Nishida *et al.*, Targeted nucleotide editing using hybrid prokaryotic and vertebrate adaptive immune systems. *Science* **353**, aaf8729 (2016).
25. A. A. Gomaa *et al.*, Programmable removal of bacterial strains by use of genome-targeting CRISPR-Cas systems. *mBio* **5**, e00928-13 (2014).
26. D. Bikard *et al.*, Exploiting CRISPR-Cas nucleases to produce sequence-specific antimicrobials. *Nat. Biotechnol.* **32**, 1146–1150 (2014).
27. R. J. Citorik, M. Mimee, T. K. Lu, Sequence-specific antimicrobials using efficiently delivered RNA-guided nucleases. *Nat. Biotechnol.* **32**, 1141–1145 (2014).
28. K. N. Lam *et al.*, Phage-delivered CRISPR-Cas9 for strain-specific depletion and genomic deletions in the gut microbiome. *Cell Rep.* **37**, 109930 (2021).
29. J. Wang, N. B. Shoemaker, G. R. Wang, A. A. Salyers, Characterization of a *Bacteroides* mobilizable transposon, NBU2, which carries a functional lincomycin resistance gene. *J. Bacteriol.* **182**, 3559–3571 (2000).
30. B. B. Lim, M. Zimmermann, N. A. Barry, A. L. Goodman, Engineered regulatory systems modulate gene expression of human commensals in the gut. *Cell* **169**, 547–558 (2017).
31. A. G. Rottinghaus, A. Ferreiro, S. R. S. Fishbein, G. Dantas, T. S. Moon, Genetically stable CRISPR-based kill switches for engineered microbes. *Nat. Commun.* **13**, 672 (2022).
32. N. P. McNulty *et al.*, Effects of diet on resource utilization by a model human gut microbiota containing *Bacteroides cellulosilyticus* WH2, a symbiont with an extensive glycobiome. *PLoS Biol.* **11**, e1001637 (2013).
33. M. C. Hibberd *et al.*, The effects of micronutrient deficiencies on bacterial species from the human gut microbiota. *Sci. Transl. Med.* **9**, eaal4069 (2017).
34. F. Stämmler *et al.*, Adjusting microbiome profiles for differences in microbial load by spike-in bacteria. *Microbiome* **4**, 28 (2016).
35. M. I. Love, W. Huber, S. Anders, Moderated estimation of fold change and dispersion for RNA-seq data with DESeq2. *Genome Biol.* **15**, 550 (2014).
36. N. Terrapon *et al.*, PULDB: The expanded database of Polysaccharide Utilization Loci. *Nucleic Acids Res.* **46**, D677–D683 (2018).
37. R. Overbeek *et al.*, The SEED and the Rapid Annotation of microbial genomes using Subsystems Technology (RAST). *Nucleic Acids Res.* **42**, D206–D214 (2014).
38. D. A. Rodionov *et al.*, Micronutrient requirements and sharing capabilities of the human gut microbiome. *Front Microbiol.* **10**, 1316 (2019).
39. W. Luo, M. S. Friedman, K. Shedden, K. D. Hankenson, P. J. Woolf, GAGE: Generally applicable gene set enrichment for pathway analysis. *BMC Bioinf.* **10**, 161 (2009).
40. A. S. Tauzin *et al.*, Functional characterization of a gene locus from an uncultured gut *Bacteroides* conferring xylo-oligosaccharides utilization to *Escherichia coli*. *Mol. Microbiol.* **102**, 579–592 (2016).
41. A. Rogowski *et al.*, Glycan complexity dictates microbial resource allocation in the large intestine. *Nat. Commun.* **6**, 7481 (2015).
42. S. K. Reddy *et al.*, A β-mannan utilization locus in *Bacteroides ovatus* involves a GH36 alpha-galactosidase active on galactomannans. *FEBS Lett.* **590**, 2106–2118 (2016).
43. V. Bågenholm *et al.*, Galactomannan catabolism conferred by a polysaccharide utilization locus of *Bacteroides ovatus*: Enzyme synergy and crystal structure of a β-Mannanase. *J. Biol. Chem.* **292**, 229–243 (2017).
44. A. S. Luis *et al.*, Dietary pectic glycans are degraded by coordinated enzyme pathways in human colonic *Bacteroides*. *Nat. Microbiol.* **3**, 210–219 (2018).
45. D. Ndeh *et al.*, Complex pectin metabolism by gut bacteria reveals novel catalytic functions. *Nature* **544**, 65–70 (2017).
46. Y. Zhu *et al.*, Mechanistic insights into a Ca2+-dependent family of alpha-mannosidases in a human gut symbiont. *Nat. Chem. Biol.* **6**, 125–132 (2010).
47. E. C. Martens *et al.*, Recognition and degradation of plant cell wall polysaccharides by two human gut symbionts. *PLoS Biol.* **9**, e1001221 (2011).
48. N. Terrapon, J. Weiner, S. Grath, A. D. Moore, E. Bornberg-Bauer, Rapid similarity search of proteins using alignments of domain arrangements. *Bioinformatics* **30**, 274–281 (2013).
49. T. Khazaei *et al.*, Metabolic multistability and hysteresis in a model aerobe-anaerobe microbiome community. *Sci. Adv.* **6**, eaba0353 (2020).
50. S. Banno, K. Nishida, T. Arazoe, H. Mitsunobu, A. Kondo, Deaminase-mediated multiplex genome editing in *Escherichia coli*. *Nat. Microbiol.* **3**, 423–429 (2018).
51. K. Zheng *et al.*, Highly efficient base editing in bacteria using a Cas9-cytidine deaminase fusion. *Commun. Biol.* **1**, 32 (2018).
52. J. Wang *et al.*, Natural variation in preparation for nutrient depletion reveals a cost–benefit tradeoff. *PLoS Biol.* **13**, e1002041 (2015).
53. T. E. Sandberg, C. J. Lloyd, B. O. Palsson, A. M. Feist, Laboratory evolution to alternating substrate environments yields distinct phenotypic and genetic adaptive strategies. *Appl. Environ. Microbiol.* **83**, e00410-17 (2017).
54. R. Debray *et al.*, Priority effects in microbiome assembly. *Nat. Rev. Microbiol.* **20**, 109–121 (2022).
55. F. Stirling *et al.*, Rational design of evolutionarily stable microbial kill switches. *Mol. Cell* **68**, 686–697 (2017).
56. L. J. Zhu, B. R. Holmes, N. Aronin, M. H. Brodsky, CRISPRseek: A bioconductor package to identify target-specific guide RNAs for CRISPR-Cas9 genome-editing systems. *PLoS One* **9**, e108424 (2014).
57. R. Simon, U. Priefer, A. Pühler, A broad host range mobilization system for in vivo genetic engineering: Transposon mutagenesis in gram negative bacteria. *Biotechnology* **1**, 784–791 (1983).
58. W. R. Whitaker, E. S. Shepherd, J. L. Sonnenburg, Tunable expression tools enable single-cell strain distinction in the gut microbiome. *Cell* **169**, 538–546 (2017).
59. H. Li, Aligning sequence reads, clone sequences and assembly contigs with BWA-MEM. arXiv [Preprint] (2013). https://arxiv.org/abs/1303.3997 (Accessed 29 June 2023).
60. P. Danecek *et al.*, Twelve years of SAMtools and BCFtools. *Gigascience* **10**, giab008 (2021).
61. Z. W. Beller *et al.*, Nutrient resource prioritization in the human gut microbiota. European Nucleotide Archive. http://www.ebi.ac.uk/ena/browser/view/PRJEB55384. Deposited 22 August 2023.
62. C. Suarez *et al.*, Inducible CRISPR-targeted 'knockdown' of human gut Bacteroides in mice reveals glycan utilization. GlycoPOST. https://glycopost.glycosmos.org/entry/GPST000298. Deposited 6 October 2022.
63. D. A. Wesener *et al.*, Inducible CRISPR-targeted "knockdown" of human gut Bacteroides in gnotobiotic mice discloses glycan utilization strategies. GlycoPOST. https://glycopost.glycosmos.org/entry/GPST000284. Deposited 20 August 2022.
64. Z. W. Beller, knockdown_manuscript_v2. Gitlab. gitlab.com/zbeller31/knockdown_manuscript_v2. Deposited 31 August 2023.
65. Z. W. Beller, metatranscriptomics_pipeline. Gitlab. gitlab.com/zbeller31/metranscriptomics_pipeline. Deposited 13 May 2023.
66. M. C. Hibberd, COPRO-Seq. Gitlab. gitlab.com/Gordon_Lab/COPRO-Seq. Deposited 10 December 2019.